

# Synthesis and Characterization of Polyaniline Emeraldine Salt: Tunable Photoluminescence and Optoelectronic Properties for Advanced Applications

Muna A. Bin Gawbah<sup>1,2</sup>, Elfatih A. Hassan<sup>3</sup>, Faiz M.B. Elshafia<sup>4,5</sup> and Ali A.S. Marouf<sup>6,\*</sup>

<sup>1</sup>Department of Physics, Faculty of Applied and Industrial Sciences, Bahri University, Khartoum, Sudan

<sup>2</sup>Physics Department, Faculty of Education, Seiyun University, Hadhramout, Yemen.

<sup>3</sup>Department of Chemistry, College of Science, Sudan University of Science and Technology, Khartoum, Sudan

<sup>4</sup>Department of Physics, Faculty of Science, Al-Baha University, Saudi Arabia

<sup>5</sup>Department of Physics, College of Science, Sudan University of Science and Technology, Khartoum, Sudan

<sup>6</sup>Department of Laser Industrial and Engineering Applications, Institute of Laser, Sudan University of Science and Technology, Khartoum, Sudan

**Abstract:** Polyaniline emeraldine salt (PANI-ES) is a conductive polymer with promising optoelectronic properties, synthesized via chemical oxidative polymerization and confirmed in its emeraldine salt form through structural analysis. Optical characterization revealed distinct absorption bands linked to key electronic transitions, indicating semiconducting behavior. Under UV excitation, photoluminescence studies showed two main emission features corresponding to dimer and excimer states, both exhibiting large Stokes shifts and a quantum yield of 0.27. These long Stokes shifts suggest efficient energy relaxation, while the moderate quantum efficiency highlights the material's capability for light-emitting applications. The combination of tunable emission, stable optical response, and electrical conductivity positions PANI-ES as a versatile material for photonic technologies. Potential applications include organic light-emitting diodes (OLEDs), photodetectors, and optically pumped organic lasers. Overall, the study demonstrates that PANI-ES offers a favorable balance of structural stability, optical performance, and electronic properties, making it a strong candidate for integration into advanced optoelectronic and photonic devices.

**Keywords:** Functional, Nanostructure, Optoelectronic, Photoluminescence, Polymerization, Semiconducting.

## 1. INTRODUCTION

Organic semiconducting laser materials (OSLMs) have garnered significant attention due to their unique advantages, such as tunable optical properties, which enable customized emission wavelengths for specific applications. Ongoing research aims to enhance their efficiency, stability, and functionality, making them a promising area of innovation in photonics and optoelectronics [1]. Among the various organic materials, conjugated polymers have emerged as a critical class of electronic materials due to their high electrical conductivity, processability, and versatile optical properties [2]. These characteristics make them highly suitable for applications such as organic light-emitting diodes (OLEDs), photodetectors, and optically pumped lasers.

Polyaniline (PANI), a prominent conjugated polymer, stands out for its ability to modulate its

electrical, optical, and chemical properties in response to external stimuli such as oxidation, protonation, and doping [3]. Its low cost, straightforward synthesis, environmental stability, and reversible doping properties make PANI a versatile material for a wide range of applications, including supercapacitors, gas sensors, biosensors, corrosion protection, energy storage systems, and solar cells [4]. The structural complexity of PANI, particularly its ability to exist in various oxidation states such as leucoemeraldine (colorless), emeraldine (blue or green), and pernigraniline (blue/violet)—further enhances its functionality. Notably, only the emeraldine salt (ES) form of PANI exhibits conductive properties, making it particularly valuable for electronic and optoelectronic applications [5].

The synthesis of PANI typically involves oxidative polymerization, where polymerization and doping occur simultaneously. This process can be achieved either electrochemically or chemically, with chemical oxidative polymerization being the most common method due to its simplicity and scalability [6]. The resulting PANI-ES

\*Address correspondence to this author at the Department of Laser Industrial and Engineering Applications, Institute of Laser, Sudan University of Science and Technology, Khartoum, Sudan; E-mail: marouf.44@gmail.com

has been extensively studied for its structural, electrical, and optical properties. In particular, its photoluminescence (PL) behavior has attracted interest due to its potential for use in optically pumped organic lasers and other photonic devices [7].

Conjugated polymers, including PANI, exhibit unique photophysical properties such as high fluorescence quantum yields and large Stokes shifts, which are advantageous for laser applications. These materials operate as intrinsic "4-level" systems, enabling high luminescence efficiencies (often exceeding 60%) and broad emission across the visible spectrum [8]. Early demonstrations of lasing in conjugated polymers by Moses [9] and subsequent studies by McGehee and Heeger [10] have highlighted their potential as efficient laser materials. Recent research has further explored the photophysical properties of conjugated polymers, including absorption spectra, fluorescence spectra, Stokes shifts, and quantum yields, to optimize their performance in optoelectronic applications [11-13].

While the photoluminescence (PL) and optoelectronic properties of polyaniline and its derivatives have been broadly explored, there remains a significant gap in the literature concerning the systematic quantification of Stokes shifts and quantum yield for polyaniline emeraldine salt (PANI-ES) synthesized via chemical oxidative polymerization, particularly under UV excitation at 325 nm. Previous studies have not comprehensively reported on the tunable PL emission and efficiency of PANI-ES in the context of its suitability for optically pumped organic laser applications. In this study, we address this gap by providing a detailed characterization of the PL properties of chemically synthesized PANI-ES, including the measurement of large Stokes shifts and quantum yield. Our findings demonstrate that PANI-ES

exhibits both substantial Stokes shifts and a moderate quantum yield, highlighting its promise as a tunable, efficient material for advanced optoelectronic and photonic devices. This work thus offers new insights into the photophysical behavior of PANI-ES and establishes its potential for integration into next-generation organic laser systems.

## 2. MATERIALS AND METHODS

### 2.1. Materials

Aniline ( $C_6H_5NH_2$ ): Obtained from Loba Chemie (India) with a purity of 99.5%, used as the monomer. Ammonium persulfate ( $(NH_4)_2S_2O_8$ ): Acquired from Central Drug House (India) with a purity of 98%, used as the oxidizing agent. Hydrochloric acid (HCl): Procured from Scharlab (Spain) with a purity of 37%, used as the dopant. Aqueous solutions were prepared using distilled water, aniline monomer, ammonium persulfate, hydrochloric acid, isopropanol, and ammonia.

### 2.2. Preparation of Polyaniline (PANI-ES)

Polyaniline (PANI) was synthesized through the chemical oxidative polymerization of aniline monomers in an acidic medium (Method 1). A flow chart of the synthetic procedures for PANI-ES is shown in Figure 1.

Figure 1 presents a schematic overview of the chemical oxidative polymerization process used to synthesize polyaniline emeraldine salt (PANI-ES). This visual representation enhances clarity and reproducibility by outlining key procedural steps, including critical control points such as temperature and pH adjustments. Displaying the synthesis workflow in a flow chart format allows readers to quickly understand the method and facilitates replication by other researchers. The figure underscores the

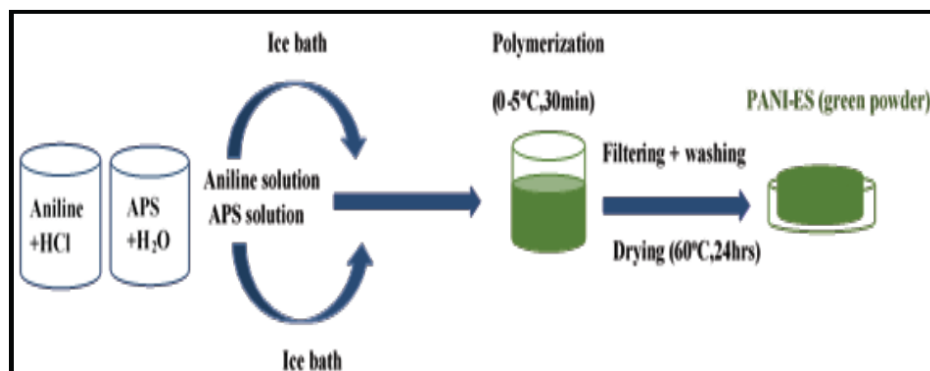


**Figure 1:** Flow chart of the chemical oxidative polymerization process for synthesizing PANI-ES, highlighting key steps such as pH adjustment (to 1.0), temperature control (0–5 °C), and dropwise addition of APS.

systematic and controlled approach employed in this study to ensure consistent synthesis of PANI-ES.

**Preparation of Aniline Solution:** mol (9.31 g) of aniline monomer was added to 100 g of 1.0 M HCl in a jacketed reaction vessel. The pH of this solution was adjusted to 1.0 with additional HCl. This highly acidic condition (pH 1.0) is essential for ensuring complete protonation of the aniline monomer, which promotes the formation of the conductive emeraldine salt form of polyaniline. Previous studies have shown that polymerization under strongly acidic conditions leads to higher conductivity and better-defined polymer structures [1]. **Preparation of Ammonium Persulfate (APS) Solution:** A solution containing 51.5 g of distilled water and 0.125 mol (28.5 g) of ammonium persulfate (APS; oxidant) was prepared in another jacketed reaction vessel. **Temperature Control:** Both solutions were placed in an ice bath at a temperature range of 0 to 5 °C. Maintaining the reaction mixture at 0–5 °C is critical to control the polymerization rate and minimize the formation of undesirable side products. Low temperatures suppress rapid oxidation and chain branching, resulting in higher molecular weight polymers with improved structural regularity and optical properties [1]. **Polymerization Reaction:** The APS solution was added drop-wise while stirring into the aniline solution. The reaction mixture was allowed to react for 30 minutes. **Isolation and Purification:** The resulting product was filtered and washed with water. The product was then dried in an oven at 60°C for 24 hours. **Final Product:** The doped form of polyaniline, PANI-ES (emeraldine salt form), was obtained as a dark green powder. The synthesized PANI-ES was ground in a mortar to obtain very fine particles [1].

### 2.3. Characterizations

**Fourier Transform Infrared Spectroscopy (FTIR):** Used to identify the functional groups of aniline (ANI) and polyaniline emeraldine salt (PANI-ES). Spectra were recorded between 4,000 and 400  $\text{cm}^{-1}$  wave numbers using an FTIR-8400S spectrophotometer (Shimadzu, Japan) with a resolution of 1  $\text{cm}^{-1}$ . The FTIR spectra were obtained using the potassium bromide (KBr) pressed disc technique. Samples were mixed with dry KBr powder at a ratio of 1:100 and pressed into disks for scanning. **UV-Visible (UV-Vis) Spectroscopy:** To measure the absorption of PANI-ES, a UV-Vis spectrophotometer (UV Mini 1240, Shimadzu, Japan) was used. The spectrophotometer covers wavelengths from 190 to 1100 nm and features an auto lamp switch from the visible to ultraviolet range.

**Photoluminescence (PL) Spectroscopy:** The PL spectrum was recorded using a He-Cd laser (KIMMON KOHA CO., LTD., Japan) operating in continuous wave (CW) mode. The laser had a wavelength of 325 nm and a maximum output power of 200 mW, used to excite light from PANI-ES.

### 2.4. Statement of Human and Animal Rights

This study did not involve human participants or animals. All experiments were conducted in compliance with ethical standards for chemical synthesis and material characterization.

## 3. RESULTS

### 3.1. FTIR Spectral Results

The FTIR spectra of the monomer aniline and the synthesized polyaniline emeraldine salt (PANI-ES) are presented in Figure 2.

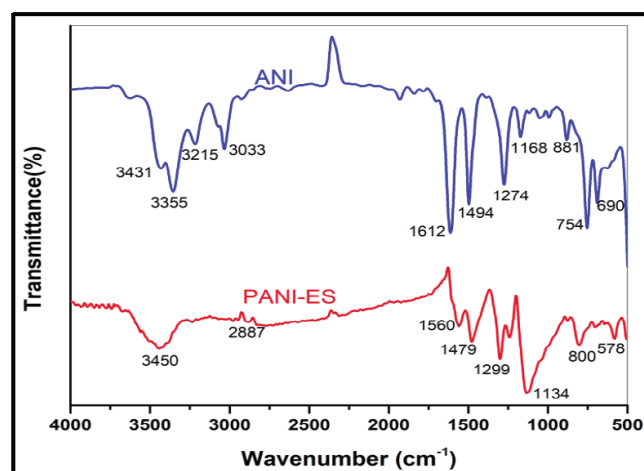


**Figure 2:** FTIR spectra of (a) aniline and (b) PANI-ES. Key vibrational modes confirm the structural transformation from aniline to the emeraldine salt form of polyaniline.

#### 3.1.1. Aniline Spectrum

The FTIR spectrum of aniline exhibits characteristic peaks corresponding to its functional groups. The N–H stretching vibrations of the primary amine group ( $\text{RNH}_2$ ) are observed as two distinct bands at 3431  $\text{cm}^{-1}$  and 3355  $\text{cm}^{-1}$ , representing asymmetric and symmetric stretching, respectively [13]. A shoulder band at 3215  $\text{cm}^{-1}$ , attributed to an overtone of the N–H bending vibration, further confirms the presence of the amine group [14]. Aromatic C–H stretching and in-plane deformation vibrations are observed at 3033  $\text{cm}^{-1}$  and 1168  $\text{cm}^{-1}$ , respectively [15]. The sharp band at 1612  $\text{cm}^{-1}$  corresponds to N–H bending vibrations of primary amines [14], while the peak at 1494  $\text{cm}^{-1}$  is assigned

to C=C ring stretching [14]. The C–N stretching vibrations are evident at  $1274\text{ cm}^{-1}$ ,  $754\text{ cm}^{-1}$ , and  $690\text{ cm}^{-1}$  [14]. Additionally, the peak at  $881\text{ cm}^{-1}$  is attributed to the out-of-plane bending of C–H [16]. These observations indicate the presence of characteristic functional groups in aniline.

### 3.1.2. PANI-ES Spectrum

The FTIR spectrum of PANI-ES reveals characteristic peaks at  $3450\text{ cm}^{-1}$ ,  $2887\text{ cm}^{-1}$ ,  $1560\text{ cm}^{-1}$ ,  $1479\text{ cm}^{-1}$ ,  $1299\text{ cm}^{-1}$ ,  $1134\text{ cm}^{-1}$ ,  $800\text{ cm}^{-1}$ , and  $578\text{ cm}^{-1}$ . The band at  $3450\text{ cm}^{-1}$  is assigned to N–H stretching of aromatic amines [17], while the peak at  $2887\text{ cm}^{-1}$  corresponds to aromatic C–H stretching [17]. The prominent bands at  $1560\text{ cm}^{-1}$  and  $1479\text{ cm}^{-1}$  are attributed to C=N and C=C stretching vibrations of quinoid and benzenoid rings, respectively [18]. The peak at  $1299\text{ cm}^{-1}$  is associated with N–H stretching of the benzenoid ring [18], and the strong band at  $1134\text{ cm}^{-1}$  is assigned to vibration modes of N=Q=N (where Q represents quinonic-type rings) [18]. The peaks at  $800\text{ cm}^{-1}$  and  $578\text{ cm}^{-1}$  are attributed to out-of-plane bending of C–H [19]. These results are consistent with previously reported FTIR spectra of polyaniline, confirming the successful conversion of aniline monomer to PANI-ES [18].

## 3.2. Optical Properties Measurements

### 3.2.1. Absorption Spectrum

The UV-Visible absorption spectrum of PANI-ES, shown in Figure 3a, exhibits three distinct absorption peaks: a sharp peak at 316 nm, a shoulder peak at 444 nm, and a broad peak spanning 700–900 nm (centered

at approximately 870 nm). The peak at 316 nm corresponds to the  $\pi$ – $\pi^*$  electron transition along the PANI backbone, while the shoulder at 444 nm is attributed to polaronic transitions (polaron– $\pi^*$ ), resulting from protonation. The broad peak around 870 nm is assigned to  $\pi$ -polaron electronic transitions [20]. These features confirm the successful doping of PANI with HCl, forming the emeraldine salt (ES) form, and are consistent with previously reported UV-Visible spectra of PANI-ES [21]. The absorption spectrum of PANI-ES is influenced by factors such as doping level, conjugation extent, polymer nature, and solvent used [22].

### 3.2.2. Optical Energy Band Gap Calculation

The optical energy band gap ( $E_g$ ) is a critical parameter that determines the material's optical absorption properties. It can be calculated using the Tauc relation [20]:

$$(\alpha h\nu)^2 = A(h\nu - E_g)^n$$

where  $\alpha$  is the absorption coefficient,  $h\nu$  is the photon energy,  $A$  is a constant, and  $n$  depends on the nature of the electronic transition. For direct band gap materials,  $n=1/2$  for allowed transitions. The direct band gap ( $E_{gd}$ ) of PANI-ES was determined using Tauc's plot by plotting  $(\alpha h\nu)^2$  versus  $h\nu$  and extrapolating the linear region to  $(\alpha h\nu)^2=0$ , as shown in Figure 3b. The calculated  $E_{gd}$  value of 3.1 eV aligns with previously reported values for PANI-ES [20], confirming its suitability for optoelectronic applications.

Figure 3b. Plot of  $(\alpha h\nu)^2$  vs. Photon Energy ( $h\nu$ ) for Determining the Direct Optical Band Gap of PANI-ES.

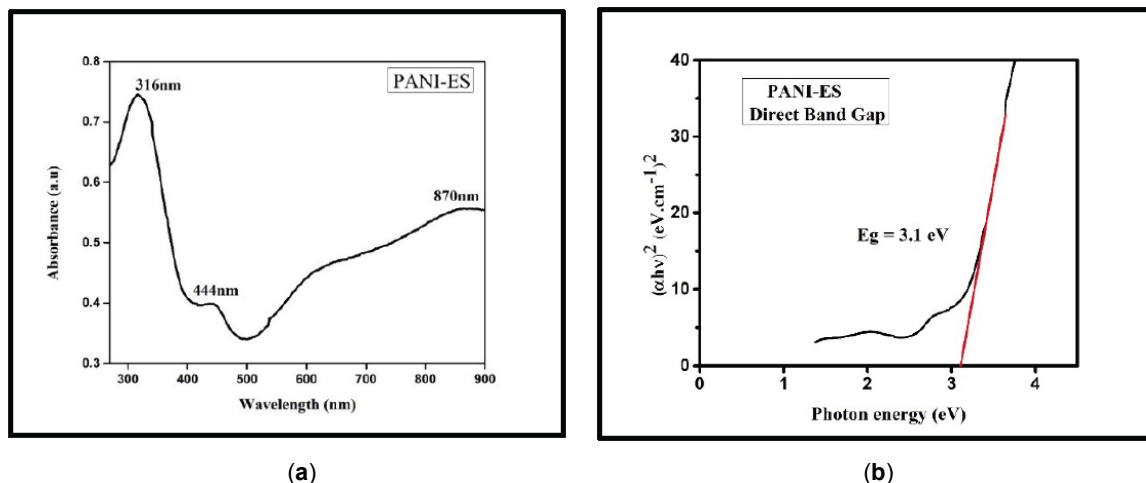


**Figure 3:** (a) UV-Vis absorption spectrum of PANI-ES showing  $\pi$ – $\pi^*$ , polaron– $\pi^*$ , and  $\pi$ -polaron transitions. (b) Tauc plot for PANI-ES showing direct optical band gap determination. The red line represents the linear fit used to extrapolate the band gap energy ( $E_g = 3.1\text{ eV}$ ). Axes are plotted as  $(\alpha h\nu)^2$  versus photon energy ( $h\nu$ ), consistent with a direct allowed transition. Note: The red line is the fitting region used in  $E_g$  estimation.

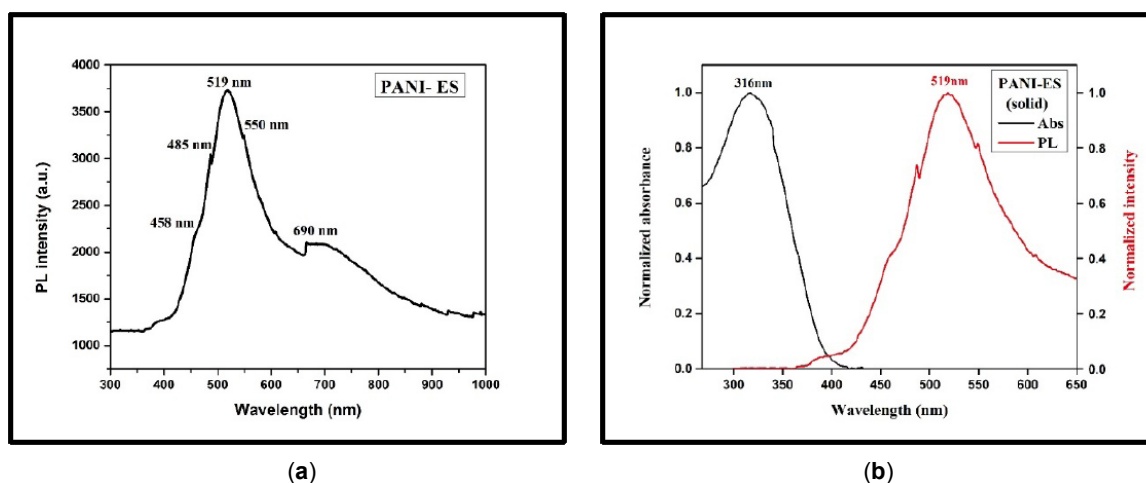


**Figure 4:** (a) PL spectrum of PANI-ES under 325 nm excitation, with emissions at 519 nm (dimer) and 690 nm (excimer), plus a shoulder at 458 nm, (b) Overlay of normalized absorption and emission spectra showing large Stokes shifts; inset shows quantum yield setup ( $\Phi = 0.27$ ).

### 3.2.3. Photoluminescence (PL)

The photoluminescence (PL) spectrum of PANI-ES, excited at 325 nm, is shown in Figure 4a. The spectrum exhibits a main emission peak at 519 nm (2.39 eV) and a broad peak around 690 nm (1.8 eV), with a small shoulder at 458 nm (2.71 eV). The intense peak at 519 nm is attributed to dimer emissions, while the broad peak at 690 nm is associated with excimer formations [21, 23]. These features confirm the semiconducting behavior of PANI-ES, as the emission peaks indicate the presence of excitons and localized states within the material.

### 3.3. Stokes' Shift and Quantum Yield

#### 3.3.1. Stokes' Shift

The Stokes shift, defined as the energy difference between the absorption and emission maxima, was calculated for PANI-ES. As shown in Figure 4b, the absorption peak at 316 nm corresponds to emission peaks at 519 nm and 690 nm, resulting in Stokes shifts of 203 nm and 374 nm, respectively. These values are consistent with previously reported Stokes shifts for polyaniline derivatives, such as the 205 nm shift observed for per-fluorinated PANI [23].

#### 3.3.2. Quantum Yield of Fluorescence

The quantum yield (QY) of PANI-ES was determined using rhodamine 6G (QY = 0.94) as a reference standard. The QY was calculated using the following equation [24]:

$$QY_S = QY_{ref} \left( \frac{\int I_S(v) d(v)}{\int I_{ref}(v) d(v)} \right) \left( \frac{OD_{ref}}{OD_S} \right) \left( \frac{n_S}{n_{ref}} \right)^2$$

where  $I_s$  and  $I_{ref}$  are the integrated fluorescence intensities of the sample and reference,  $OD_s$  and  $OD_{ref}$  are the optical densities, and  $n_s$  and  $n_{ref}$  are the refractive indices of the solvents. The calculated QY of PANI-ES was 0.27, which is comparable to values reported for other conjugated polymers, such as poly(9,9-dioctylfluorenyl-2,7-diyl) (PFO) and poly[9,9-di-(2-ethylhexyl)fluorenyl-2,7-diyl] (PDHF) [24].

## 4. DISCUSSION

The successful synthesis of polyaniline emeraldine salt (PANI-ES) was confirmed through FTIR analysis, which revealed characteristic peaks corresponding to N–H stretching, C–H stretching, and C=N/C=C vibrations in the quinoid and benzenoid rings. These findings are consistent with previous studies, validating the structural transformation from aniline to PANI-ES [18]. The UV-Visible absorption spectrum further supports this conclusion, displaying three distinct peaks at 316 nm, 444 nm, and 870 nm. These peaks are attributed to  $\pi$ - $\pi^*$ , polaron- $\pi^*$ , and  $\pi$ -polaron transitions, respectively, confirming the successful doping of PANI with HCl to form the emeraldine salt (ES) phase [20, 21]. The calculated optical band gap of 3.1 eV aligns with the semiconducting behavior of PANI-ES, underscoring its suitability for optoelectronic applications [20].

The photoluminescence (PL) spectrum of PANI-ES, excited at 325 nm, exhibits a main emission peak at 519 nm and a broad peak at 690 nm. These emissions are attributed to dimer and excimer formations, respectively, highlighting the material's semiconducting nature and the presence of excitons and localized



**Table 1: Comparison of Stokes Shift, Optical Band Gap, and Quantum Yield of Synthesized PANI-ES with Published Values for Similar Polyaniline and Conjugated Polymer Systems**

Material/System	Stokes Shift (nm)	Band Gap (eV)	Quantum Yield	Reference
This work (PANI-ES)	203, 374	3.1	0.27	[This study]
Perfluorinated PANI-ES	~205	—	—	[23]
PDHF in various solvents	—	—	0.27–0.43	[25]
Fluorescent PANI nanoparticles (aqueous solution)	—	—	$1.9 \times 10^{-3} - 6.9 \times 10^{-3}$	[26]
PANI films on electrode surfaces	—	—	$10^{-4} - 10^{-3}$	[27]
PANI–Al <sub>2</sub> O <sub>3</sub> nanocomposite	—	3.16	—	[20]

states [21, 23]. The observed Stokes shifts of 203 nm and 374 nm further emphasize the material's potential for optoelectronic applications, as they indicate efficient energy relaxation processes [23]. Additionally, the measured quantum yield of 0.27, which is comparable to other conjugated polymers, suggests that PANI-ES could be a promising candidate for light-emitting devices and laser media [25]. However, these assignments are based solely on steady-state PL spectra. No supporting data, such as time-resolved or temperature-dependent PL measurements, were collected to directly confirm the involvement of dimeric or excimeric states. This represents a limitation of the current study, and future work should include such measurements to provide more definitive evidence for the origin of these emission features.

To contextualize the optical properties of our synthesized PANI-ES, Table 1 compares its Stokes shift, optical band gap, and quantum yield with values reported for similar polyaniline systems and other conjugated polymers.

As shown, the Stokes shifts and quantum yield of our PANI-ES are comparable to or greater than those reported for similar systems, confirming its strong potential for optoelectronic and photonic applications.

The synthesis and characterization of PANI-ES reveal its nanoscale features, such as dimer and excimer formation, which are critical to its photoluminescence and optoelectronic properties. These features, combined with its tunable optical and electronic behavior, make PANI-ES a versatile material for advanced applications. Specifically, its semiconducting properties, efficient energy relaxation processes, and relatively high quantum yield position it as a strong candidate for use in organic light-emitting diodes (OLEDs), photodetectors, and optically pumped lasers.

The results of this study demonstrate the potential of PANI-ES as a functional material for optoelectronic applications. Its tunable photoluminescence, semiconducting behavior, and efficient energy relaxation processes make it a promising candidate for next-generation devices. PANI-ES is a versatile material with tunable properties, suitable for advanced applications. Further research is recommended to explore its practical implementation in OLEDs, photodetectors, and other optoelectronic systems, as well as to optimize its properties for specific applications.

While FTIR, UV-Vis, and PL spectroscopy provided comprehensive information about the chemical structure and optical properties of PANI-ES, additional analyses such as X-ray diffraction (XRD) and electron microscopy (SEM/TEM) would offer valuable insights into the material's crystallinity and nanoscale morphology. Incorporating these techniques in future studies would help to further elucidate the structural features that underpin the observed photophysical behavior, thereby strengthening the case for PANI-ES in advanced optoelectronic applications.

## 5. CONCLUSION

This study demonstrates that polyaniline emeraldine salt (PANI-ES), synthesized via chemical oxidative polymerization, exhibits a direct optical band gap of 3.1 eV and strong photoluminescence with large Stokes shifts and a quantum yield of 0.27. These optical properties indicate efficient energy relaxation and stable emission, underscoring the material's suitability for optoelectronic and photonic devices. The combination of tunable emission, moderate quantum efficiency, and electrical conductivity makes PANI-ES a promising candidate for applications such as organic light-emitting diodes (OLEDs), photodetectors, and optically pumped organic lasers. Overall, PANI-ES offers a compelling balance of structural stability,

optical performance, and electronic functionality for integration into advanced optoelectronic technologies.

## ACKNOWLEDGEMENTS

The authors gratefully acknowledge the support and assistance provided by the members of the research laboratory at Sudan University of Science and Technology during the preparation and execution of the experiments. Special thanks are extended to the laser department at Al-Neelain University for their invaluable assistance with UV-Vis spectroscopy measurements, including instrument calibration. Their contributions were instrumental in the successful completion of this work.

## FUNDING

This research did not receive any specific grant from funding agencies in the public, commercial, or not-for-profit sectors.

## CONFLICT OF INTEREST

The authors declare that they have no known competing financial interests or personal relationships that could have appeared to influence the work reported in this paper.

## ETHICS APPROVAL

Not applicable.

## CONSENT

Not applicable.

## DATA AVAILABILITY STATEMENT

All data generated or analyzed during this study are included in this published article. Raw spectral data (FTIR, UV-Vis, and photoluminescence) will be deposited in a public repository upon publication. Additional datasets are available from the corresponding author upon reasonable request.

## ETHICAL STATEMENT

This study did not involve human participants or animals. All experimental procedures were conducted in accordance with relevant ethical standards for chemical research.

## AUTHORS' CONTRIBUTIONS

Muna A. Bin Gawbah: Conceptualization, Methodology, Investigation, Writing – Original Draft.

Elfatih A. Hassan: Formal Analysis, Validation, Writing – Review & Editing, Supervision, Project Administration.

Faiz M. B. Elshafia: Resources, Data Curation, Visualization.

Ali A. S. Marouf: Writing – Review & Editing, Supervision, Project Administration.

All authors read and approved the final manuscript.

## REFERENCES

- [1] Müllen K, Reynolds JR, Masuda T, editors. *Conjugated polymers: a practical guide to synthesis*. London: R Soc Chem; 2013.  
<https://doi.org/10.1039/9781849739771-FP013>
- [2] Zhu A, Zhang J, Situ B, *et al.* Preparation of polyaniline@graphene nanocomposite with oxidative polymerization of pre-assembled of aniline for supercapacitor electrodes. *J Polym Res* 2023; 30: 417.  
<https://doi.org/10.1007/s10965-023-03794-4>
- [3] Fang XB, Hong B, Xu JC, *et al.* Highly-improved high-frequency and broadband microwave absorption performance of polyaniline coated SrCo<sub>2</sub>Z hexaferrites. *J Mater Res* 2024; 39: 1-13.  
<https://doi.org/10.1557/s43578-024-01500-8>
- [4] Babel V, Hiran BL. A review on polyaniline composites: synthesis, characterization, and applications. *Polym Compos* 2021; 42: 3142-57.  
<https://doi.org/10.1002/pc.26048>
- [5] MacDiarmid A, Chiang J, Richter A, *et al.* Polyaniline: a new concept in conducting polymers. *Synth Met* 1987; 18: 285-90.  
[https://doi.org/10.1016/0379-6779\(87\)90893-9](https://doi.org/10.1016/0379-6779(87)90893-9)
- [6] Goswami S, Nandy S, Fortunato E, Martins R. Polyaniline and its composites engineering: a class of multifunctional smart energy materials. *J Solid State Chem* 2023; 317: 123679.  
<https://doi.org/10.1016/j.jssc.2022.123679>
- [7] Latypova LR, Usmanova GS, Vasilova LY, *et al.* Synthesis of N-alkyl- and N-alkenyl-substituted polyanilines. Properties and antibacterial activity study. *J Polym Res* 2023; 30: 315.  
<https://doi.org/10.1007/s10965-023-03696-5>
- [8] Nara M, Orita R, Ishige R, Ando S. White-light emission and tunable luminescence colors of polyimide copolymers based on FRET and room-temperature phosphorescence. *ACS Omega* 2020; 5: 14831-41.  
<https://doi.org/10.1021/acsomega.0c01949>
- [9] Almarashi JQM, Gadallah A-S, Ellabban MA, Mohamed AH. Improvement of MEH-PPV performance for laser and optoelectronic applications. *Opt Mater* 2024; 150: 115240.  
<https://doi.org/10.1016/j.optmat.2024.115240>
- [10] Ly HQ, Chen YJ, Nguyen VT, Tseng CL. Optimization of the poloxamer 407-conjugated gelatin to synthesize pH-sensitive nanocarriers for controlled paclitaxel delivery. *J Polym Res* 2025; 32: 14.  
<https://doi.org/10.1007/s10965-024-04248-1>
- [11] Barros HL, Esteves MA, Brites MJ. Synthesis, photophysical and electrochemical properties of  $\pi$ -conjugated pyrene based down-shifting molecules with fluorinated aryl groups. *Dyes Pigm* 2023; 213: 111103.  
<https://doi.org/10.1016/j.dyepig.2023.111103>
- [12] Elshaikh M, Marouf AAS, Ibnaouf KH. Desirable amplified spontaneous emission (ASE) from a conjugated polymer

- poly(9,9-dioctylfluorenyl-2,7-diyl) end capped with 2,5-diphenyl-1,2,4-oxadiazole (PFO) in liquid and solid state. *Int J Adv Res Phys Sci* 2019; 6: 7-15.
- [13] Elshaikh M, Marouf AA, Modwi A, Ibnaouf KH. Influence of the organic solvents on the  $\alpha$  and  $\beta$  phases of a conjugated polymer (PFO). *Dig J Nanomater Biostruct* 2019; 14: 1069-77.
- [14] Yadav L. Infrared (IR) spectroscopy. In: *Organic spectroscopy*. Dordrecht: Springer; 2005. p. 52-106. <https://doi.org/10.1007/978-1-4020-2575-4>
- [15] Huang C, Li A, Li L-J, Chao Z-S. Synthesis of quinolines from aniline and propanol over modified USY zeolite: catalytic performance and mechanism evaluated by in situ Fourier transform infrared spectroscopy. *RSC Adv* 2017; 7: 24950-62. <https://doi.org/10.1039/C7RA04526C>
- [16] Anwer T, Ansari MO, Mohammad F. Morphology and thermal stability of electrically conducting nanocomposites prepared by sulfosalicylic acid micelles assisted polymerization of aniline in presence of  $ZrO_2$  nanoparticles. *Polym Plast Technol Eng* 2013; 52: 472-7. <https://doi.org/10.1080/03602559.2012.757624>
- [17] Sengupta PP, Barik S, Adhikari B. Polyaniline as a gas-sensor material. *Mater Manuf Process* 2006; 21: 263-70. <https://doi.org/10.1080/10426910500464602>
- [18] Gairola S, Verma V, Kumar L, *et al.* Enhanced microwave absorption properties in polyaniline and nano-ferrite composite in X-band. *Synth Met* 2010; 160: 2315-8. <https://doi.org/10.1016/j.synthmet.2010.08.025>
- [19] Yao F, Xie W, Yang M, *et al.* Interfacial polymerized copolymers of aniline and phenylenediamine with tunable magnetoresistance and negative permittivity. *Mater Today Phys* 2021; 21: 100502. <https://doi.org/10.1016/j.mtphys.2021.100502>
- [20] Resan SA, Essa AF. Preparation and study of the optical properties for polyaniline- $Al_2O_3$  nanocomposite. *Mater Today Proc* 2021; 45: 5819-22. <https://doi.org/10.3390/polym13162787>
- [21] Hassan H, Sunny MA, Iqbal MW, *et al.* Study of the electrochemical properties of polyaniline-integrated chromium oxide composite with metal-organic framework electrode ( $Cr_2O_3/Sn-MOF$  (PANI)) for asymmetric supercapacitors and hydrogen production applications. *J Mater Res* 2024; 39: 1-14. <https://doi.org/10.1557/s43578-024-01495-2>
- [22] Dhivya C, Vandarkuzhali SAA, Radha N. Antimicrobial activities of nanostructured polyanilines doped with aromatic nitro compounds. *Arab J Chem* 2019; 12: 3785-98.
- [23] Dallas P, Rašović I, Puchtler T, Taylor RA, Porfyrakis K. Long Stokes shifts and vibronic couplings in perfluorinated polyanilines. *Chem Commun* 2017; 53: 2602-5. <https://doi.org/10.1039/C7CC00471K>
- [24] AlSalhi MS, Almotiri AR, Prasad S, *et al.* A temperature-tunable thiophene polymer laser. *Polymers (Basel)* 2018; 10: 470. <https://doi.org/10.3390/polym10050470>
- [25] Ibnaouf K. Amplified spontaneous emission spectra of poly(9,9-dioctylfluorenyl-2,7-diyl) under pulsed laser excitation. *Synth Met* 2015; 209: 534-43. <https://doi.org/10.1016/j.synthmet.2015.09.005>
- [26] Alves KGB, de Melo EF, Andrade CAS, de Melo CP. Preparation of fluorescent polyaniline nanoparticles in aqueous solutions. *J Nanopart Res* 2013; 15: 1-11. <https://doi.org/10.1007/s11051-012-1339-x>
- [27] Antonel PS, Andrade EM, Molina FV. Fluorescence of polyaniline films on electrode surfaces: thickness dependence and surface influence. *J Electroanal Chem* 2009; 632: 72-9. <https://doi.org/10.1016/j.jelechem.2009.03.017>

Received on 15-05-2025

Accepted on 10-06-2025

Published on 10-07-2025

<https://doi.org/10.6000/1929-5995.2025.14.09>© 2025 Gawbah *et al.*

This is an open-access article licensed under the terms of the Creative Commons Attribution License (<http://creativecommons.org/licenses/by/4.0/>), which permits unrestricted use, distribution, and reproduction in any medium, provided the work is properly cited.